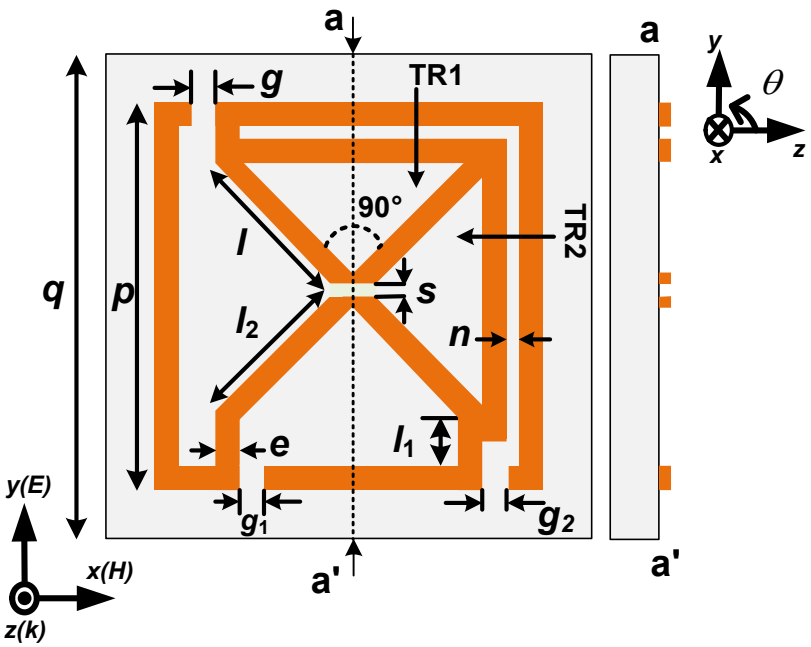

(a)

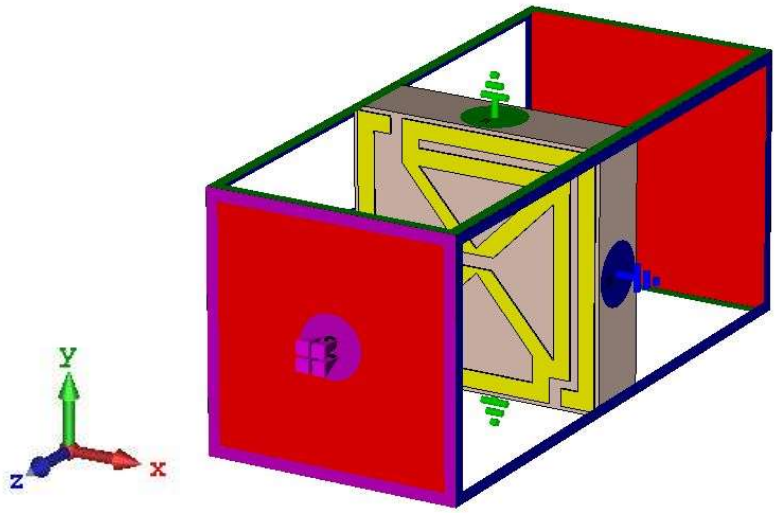

(b)

Fig. 1 Geometry of the proposed multi-band MTM unit cell. (a) Schematic layout and cross-sectional views (aa') (b) Simulation setup.

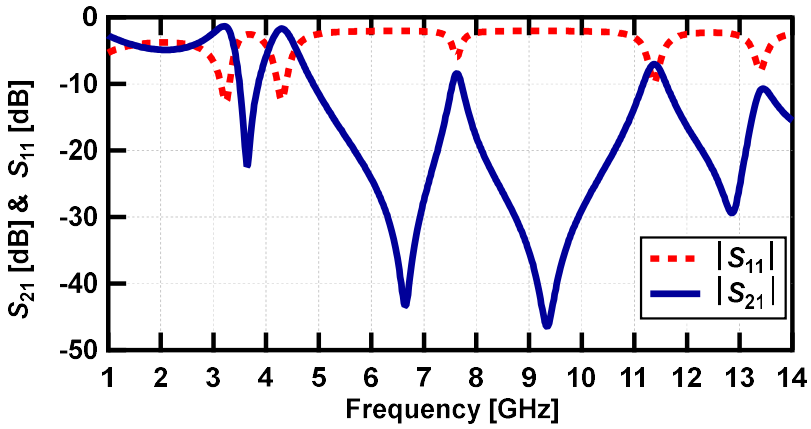

Fig. 2 Reflection (S_{11}) and transmission coefficient curves (S_{21}) of the proposed MTM unit cell.

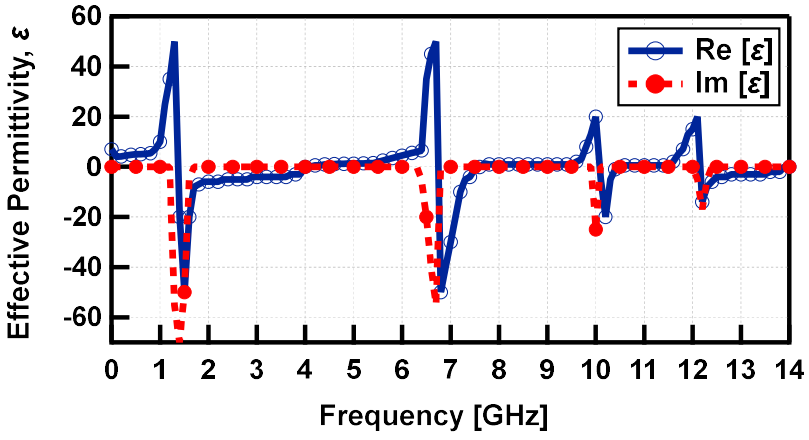

(a)

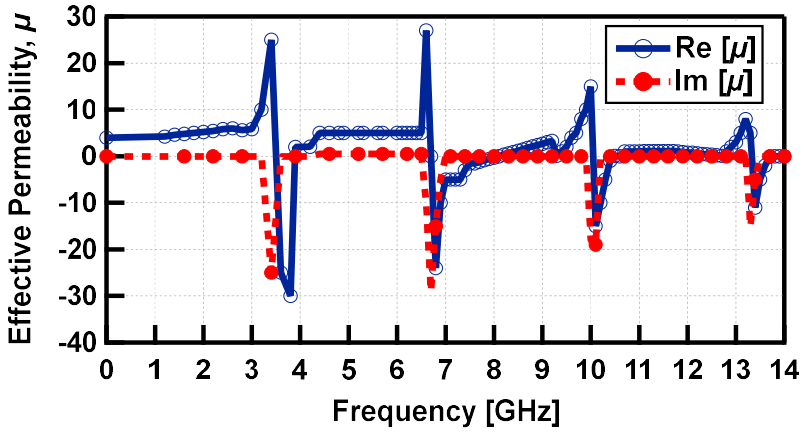

(b)

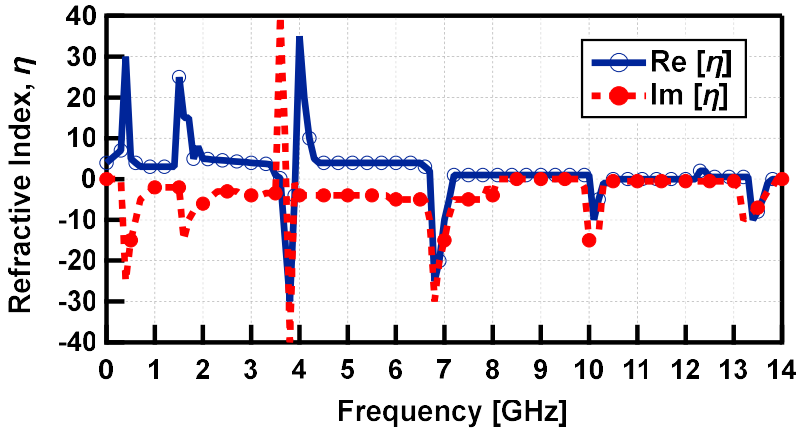

(c)

Fig. 3 Effective parameters of the proposed metamaterial unit cell: Real and imaginary values of (a) permittivity, (b) permeability, (c) refractive index.

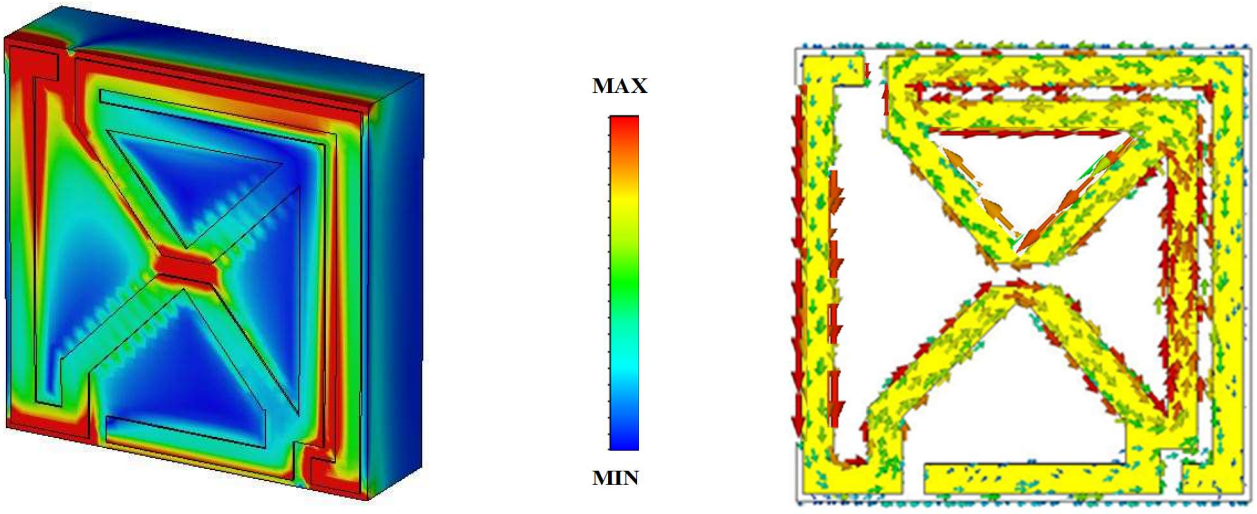

Fig. 4 (a) Localization of electric field and (b) Distribution of surface current at 3.75 GHz.

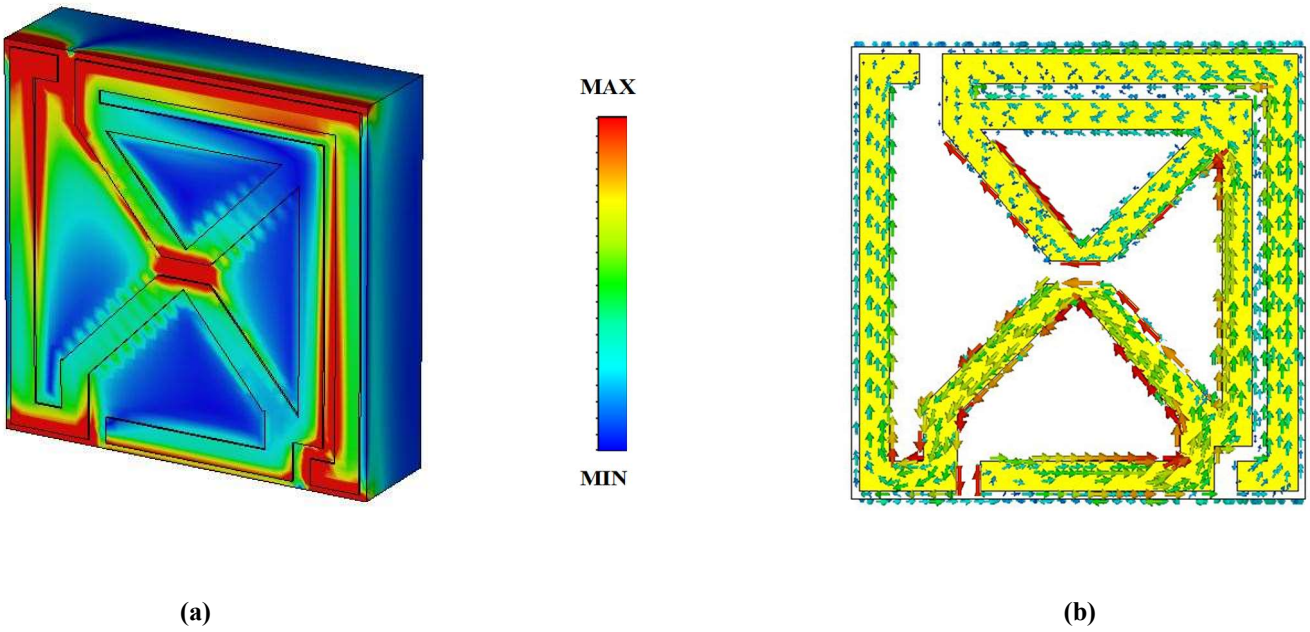

Fig. 5 (a) Localization of electric field and (b) Distribution of surface current at 6.95 GHz.

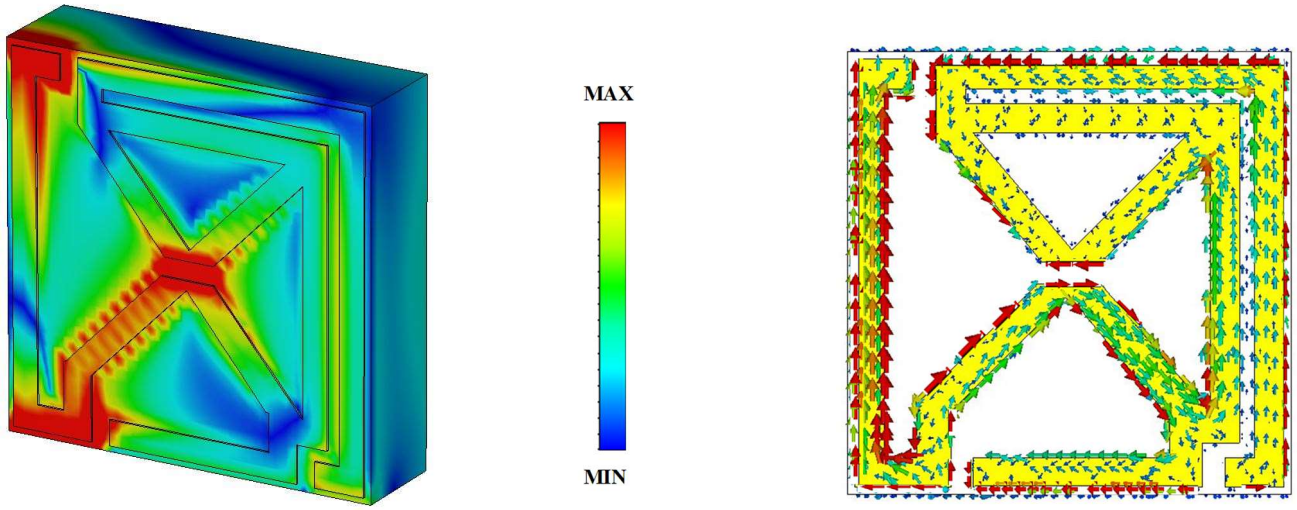

Fig. 6 (a) Localization of electric field and (b) Distribution of surface current at 10.25 GHz.

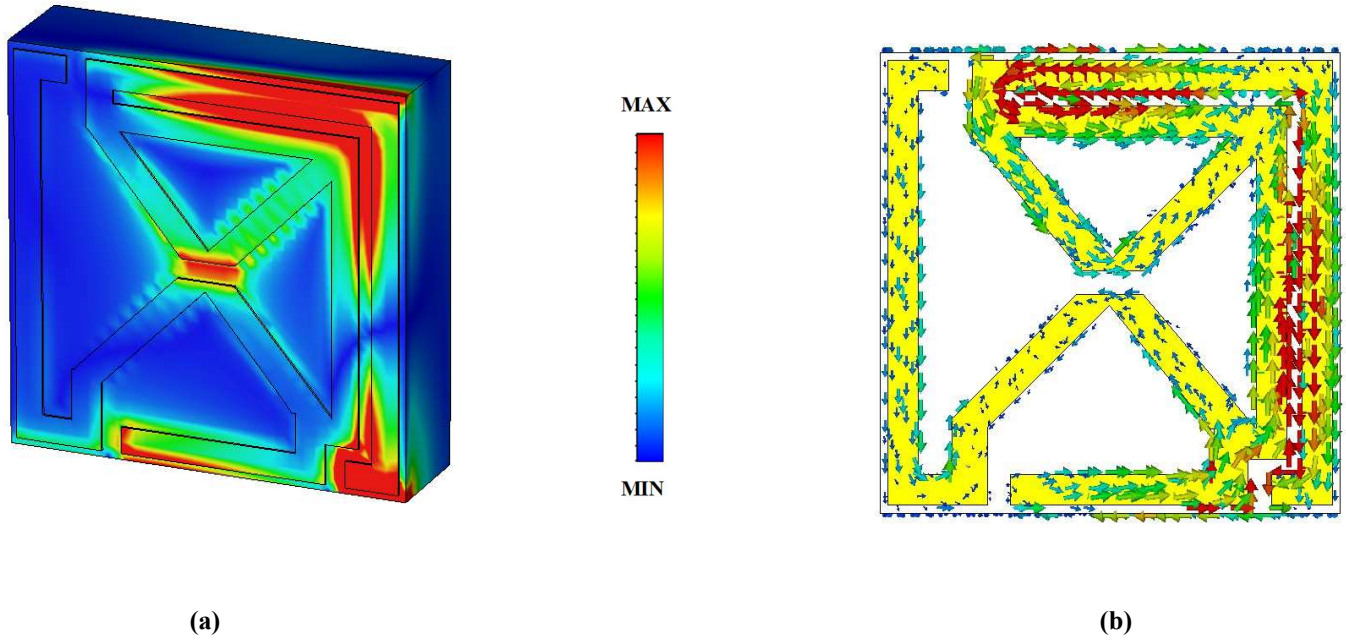

Fig. 7 (a) Localization of electric field and (b) Distribution of surface current at 13.55 GHz.

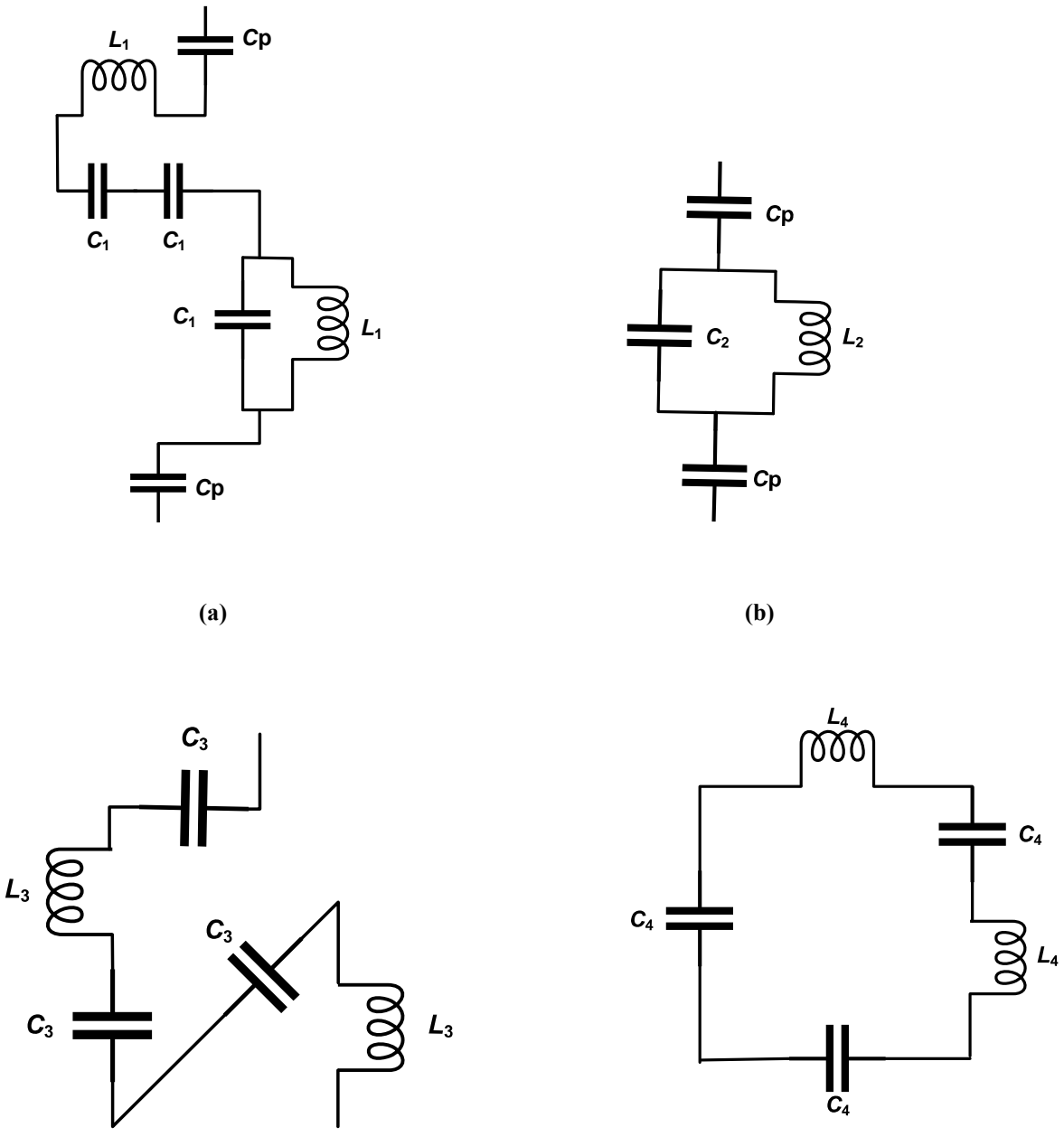

Fig. 8 Equivalent circuit at (a) 3.75 GHz, (b) 6.95 GHz, (c) 10.25 GHz, and (d) 13.55 GHz.

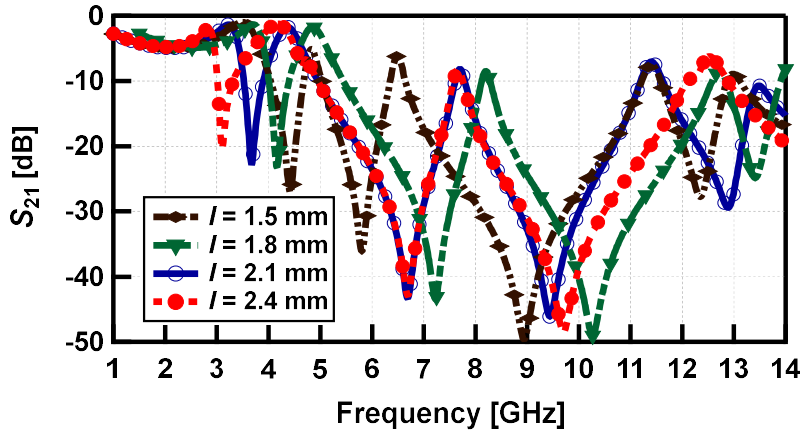

(a)

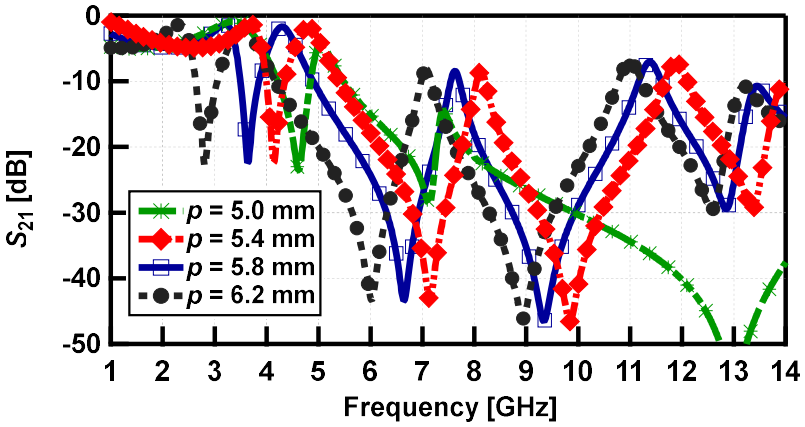

(b)

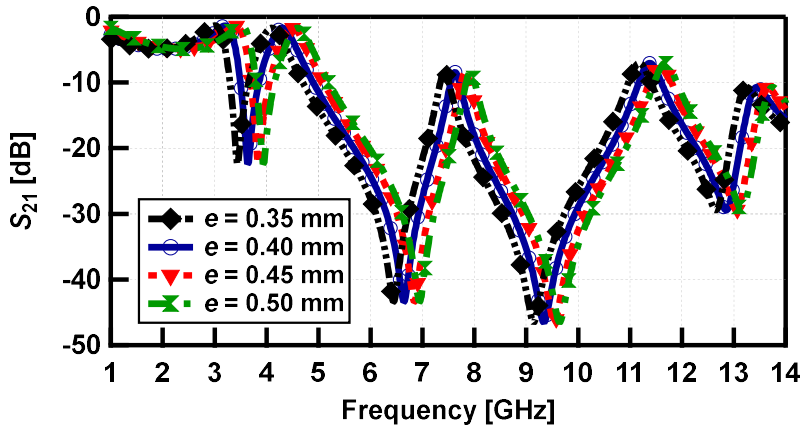

(c)

Fig. 9 Analysis of the proposed MTMs basic parameters by varying (a) *l*, (b) *p,* and (c) *e*.

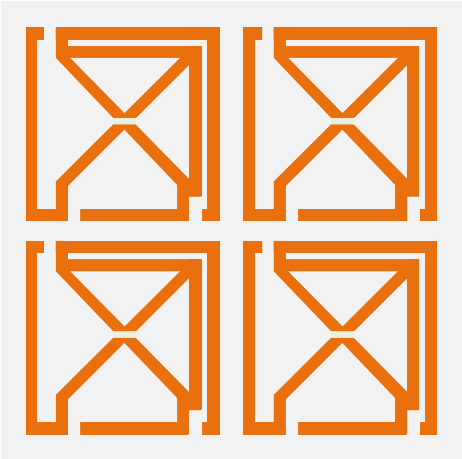

(a)

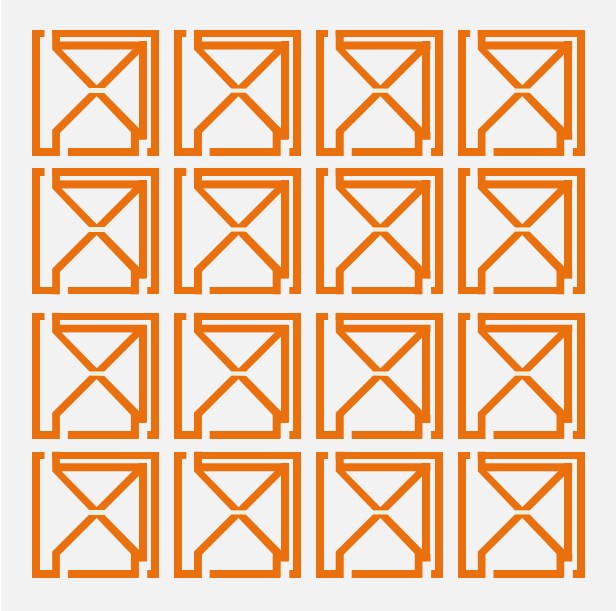

(b)

Fig. 10 Arrangement of arrays designed by employing the proposed MTM unit cell. (a) 2×2 and (b) 4×4.

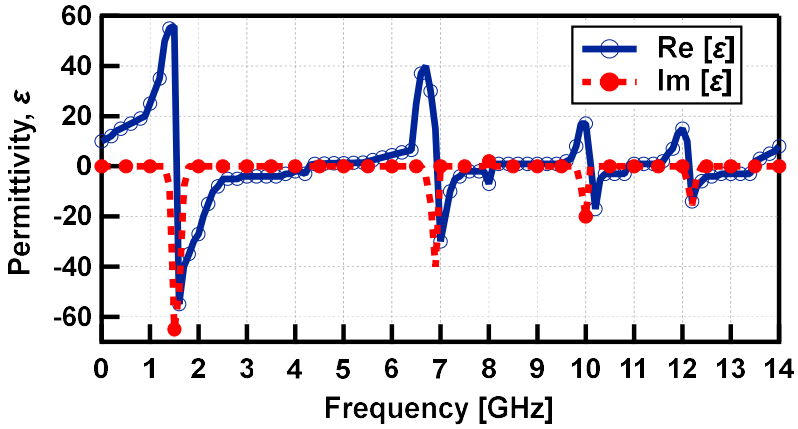

(a)

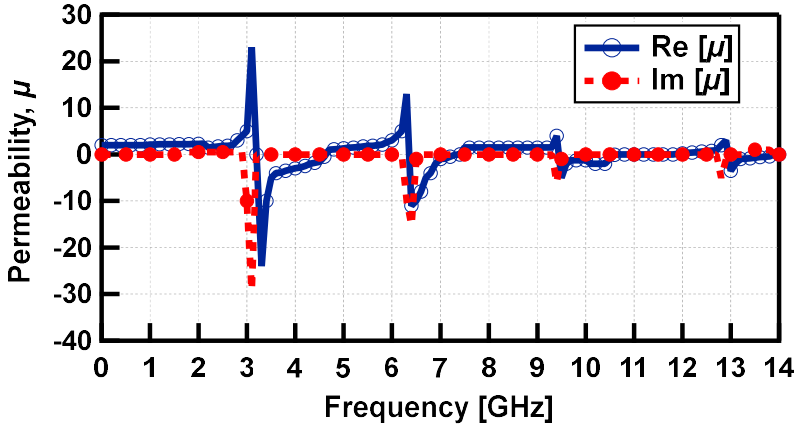

(b)

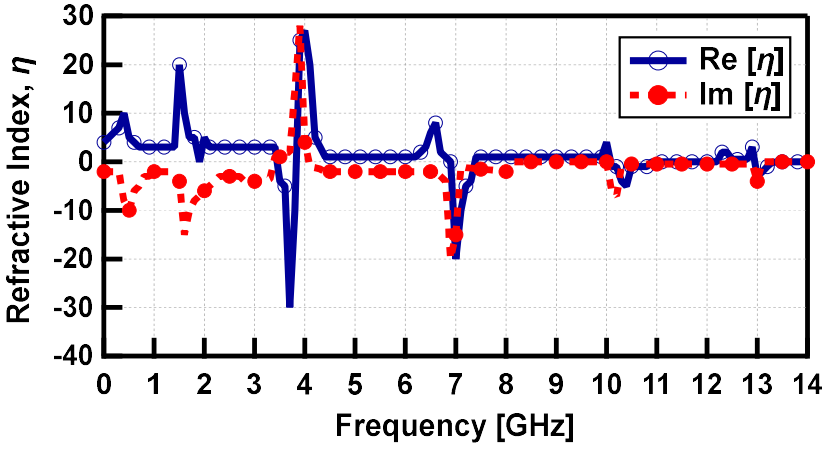

(c)

Fig. 11 Effective parameters of the 2×2 array. (a) ε, (b) μ, and (c) η.

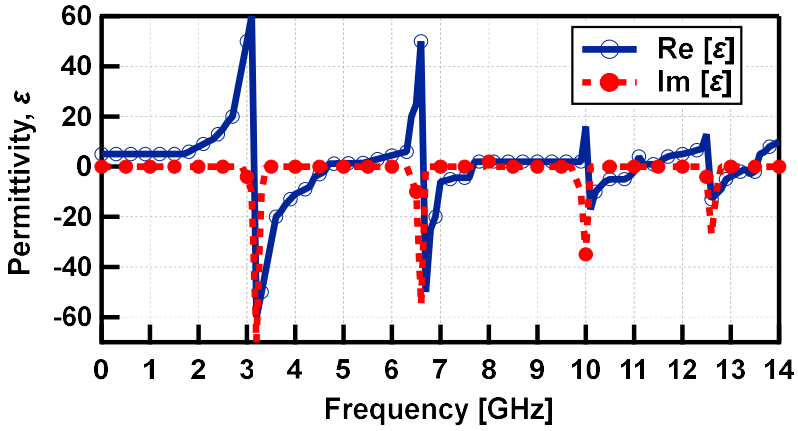

(a)

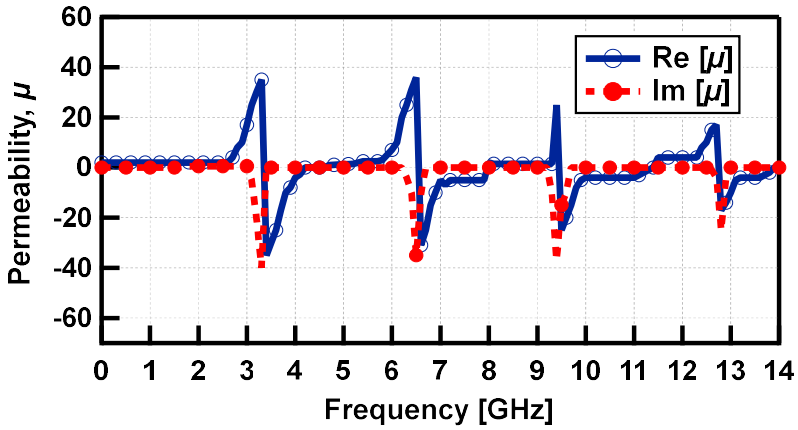

(b)

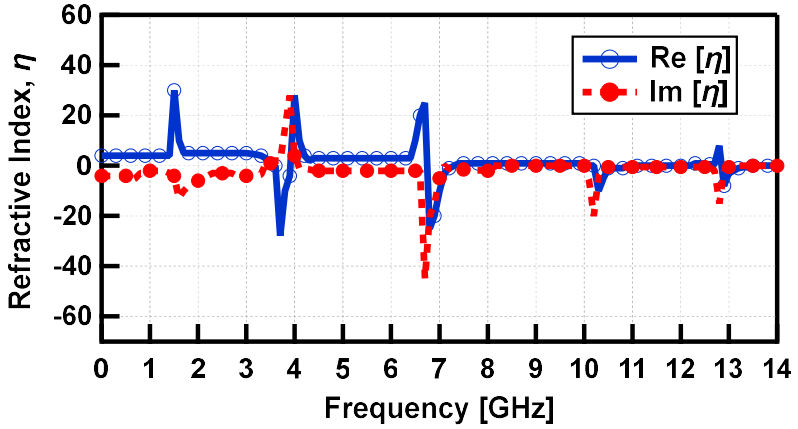

(c)

Fig. 12 Effective parameters of the 4×4 array. (a) ε, (b) μ, and (c) η.

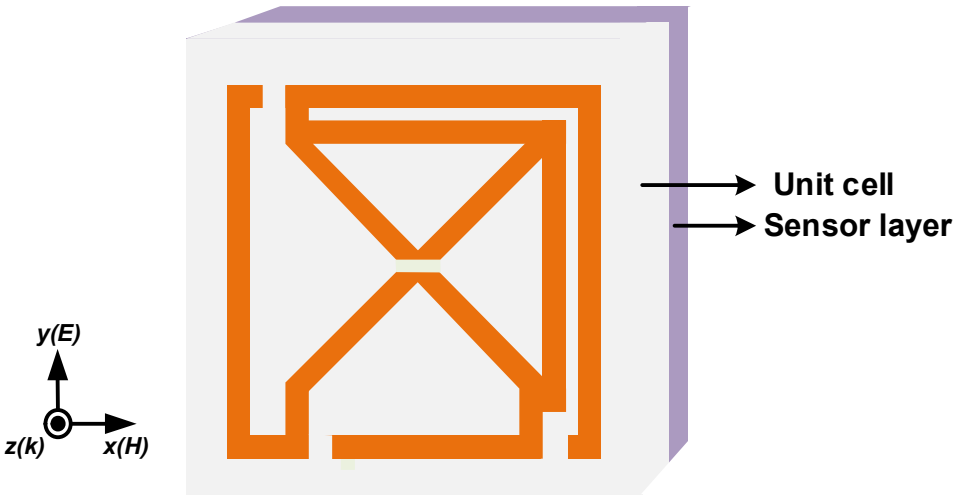

(a)

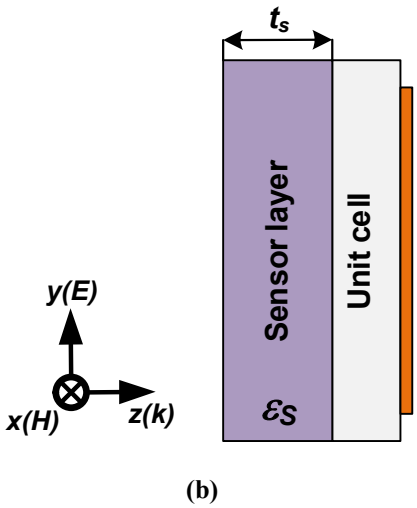

(b)

Fig. 13 Schematic diagram of the proposed unit cell-based transformer oil aging sensor. (a) Perspective view and (b) Left view.

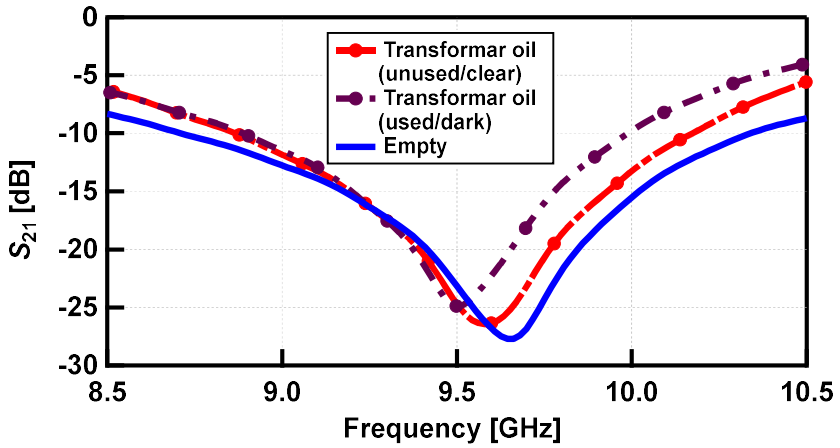

Fig. 14 Simulated transmission coefficients of the proposed unit cell-based transformer oil aging sensor.

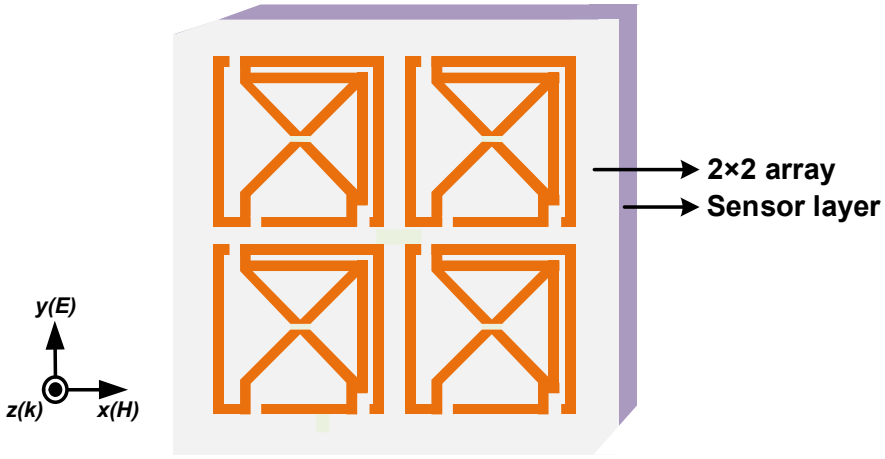

(a)

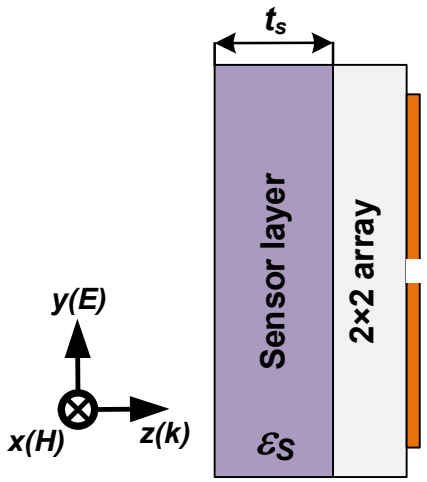

(b)

Fig. 15 Schematic diagram of the proposed 2×2 MTM array-based transformer oil aging sensor. (a) Perspective view and (b) Left view.

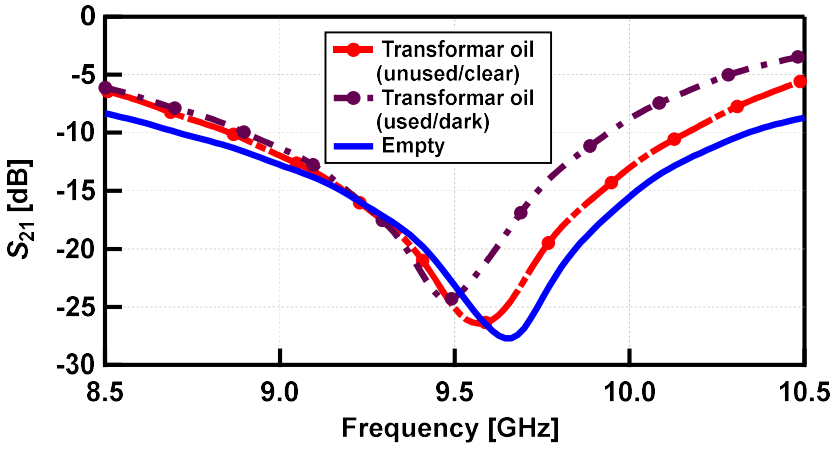

Fig. 16 Simulated transmission coefficients of clear and dark transformer oil.

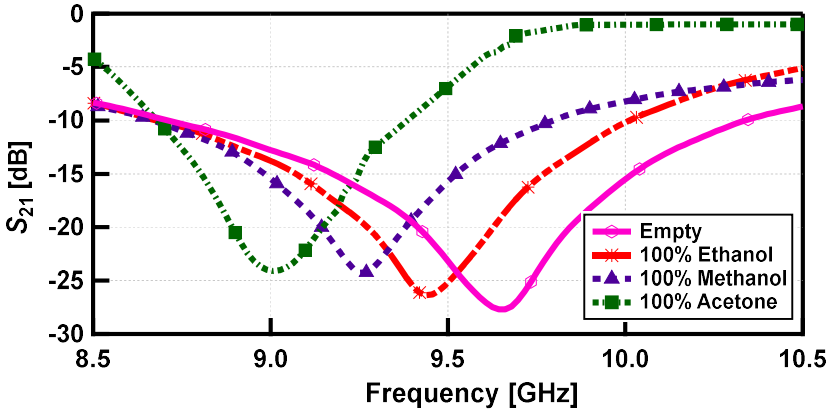

Fig. 17 S_{21} curves of the multipurpose chemical sensor.

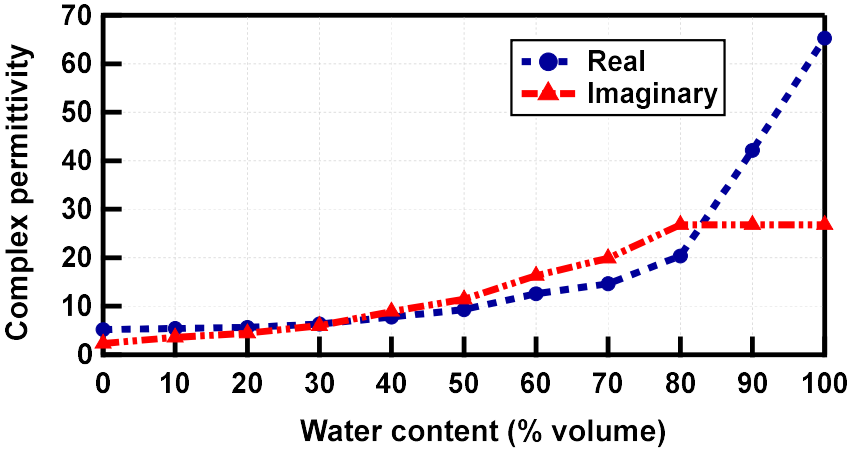

(a)

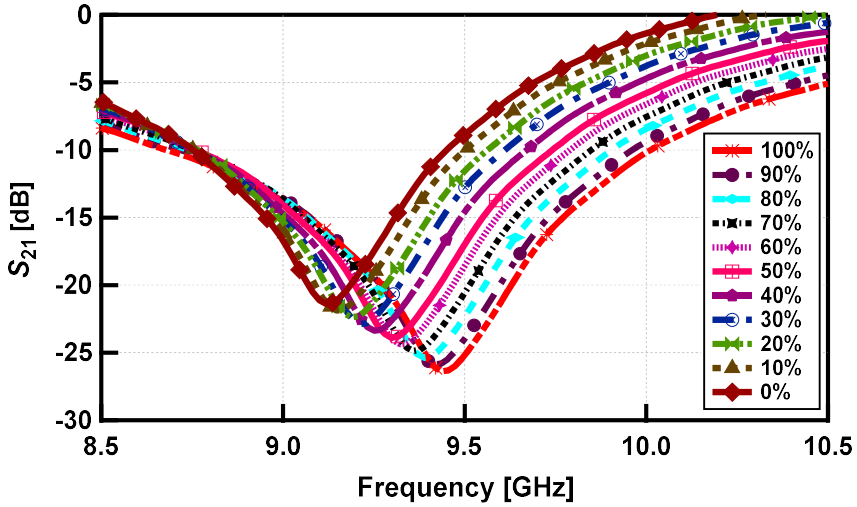

(b)

Fig. 18 (a) Complex permittivity of ethanol-water mixture when the water content increases from 0% to 100% with a step of 10% by volume. (b) Simulated transmission coefficient curves for ethanol-water mixture when the ethanol content increases from 0% to 100%.

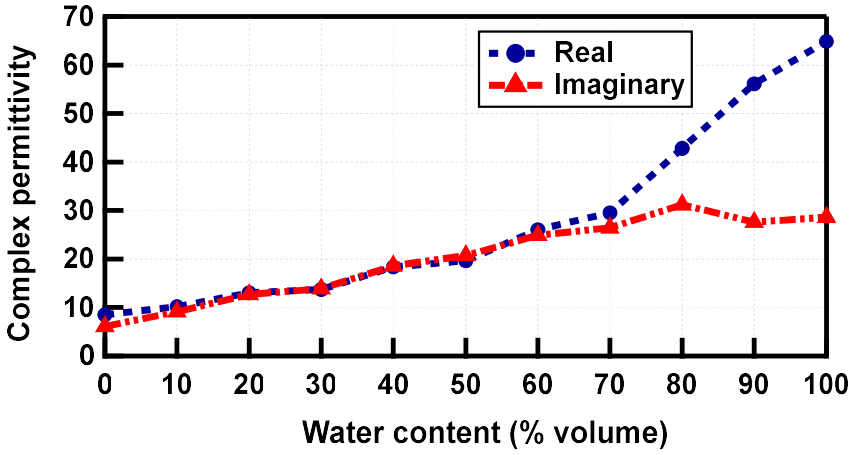

(a)

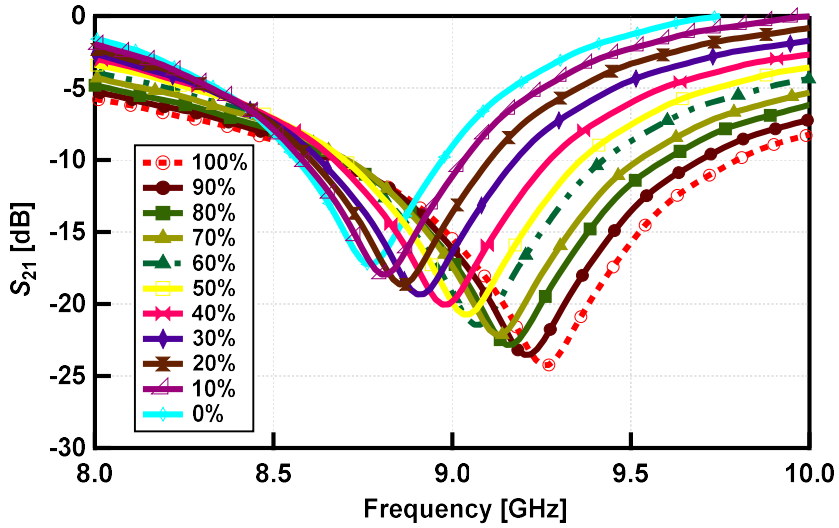

(b)

Fig. 19 (a) Complex permittivity of methanol-water mixture when the water content increases from 0% to 100% with a step of 10% by volume. (b) Simulated transmission coefficient curves for methanol-water mixture when the methanol content increases from 0% to 100%.

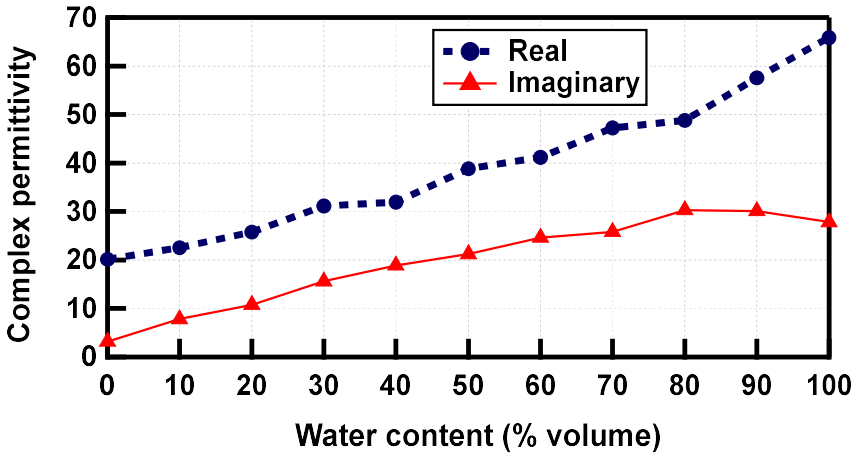

(a)

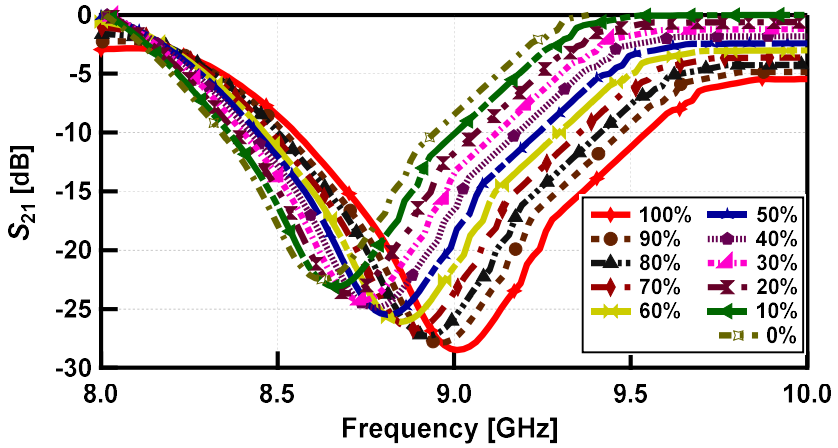

(b)

Fig. 20 (a) Complex permittivity of acetone-water mixture when the water content increases from 0% to 100% with a step of 10% by volume. (b) Simulated transmission coefficient for acetone-water mixture when the acetone content increases from 0% to 100%.

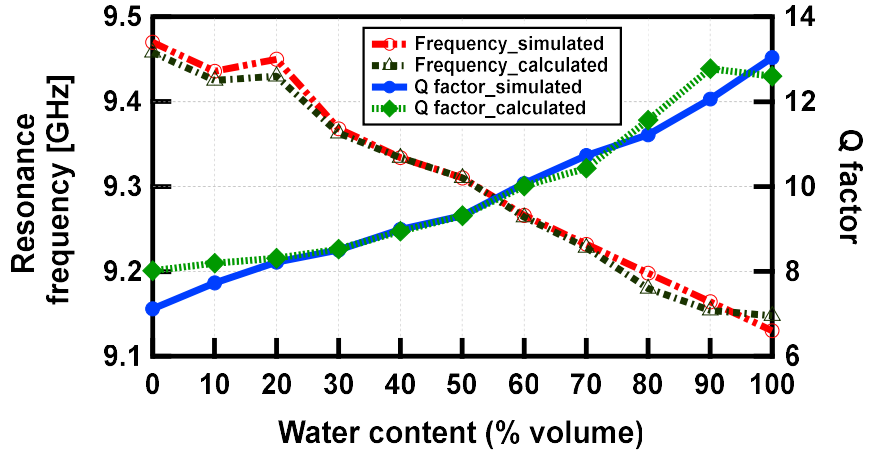

(a)

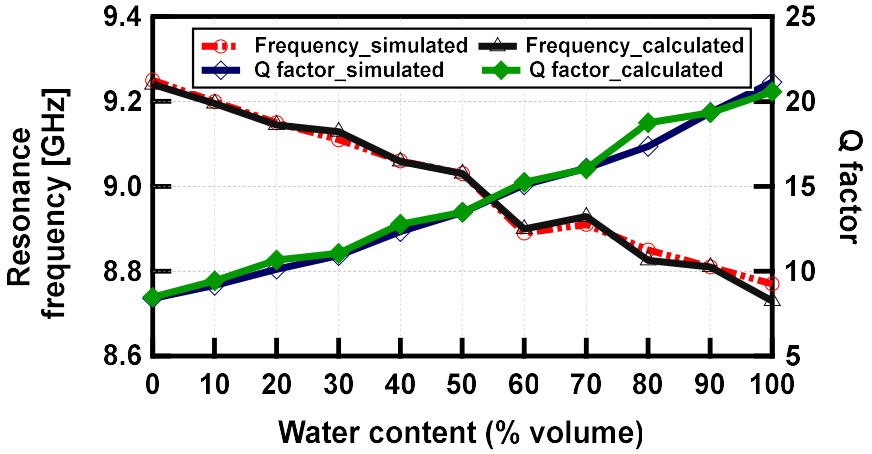

(b)

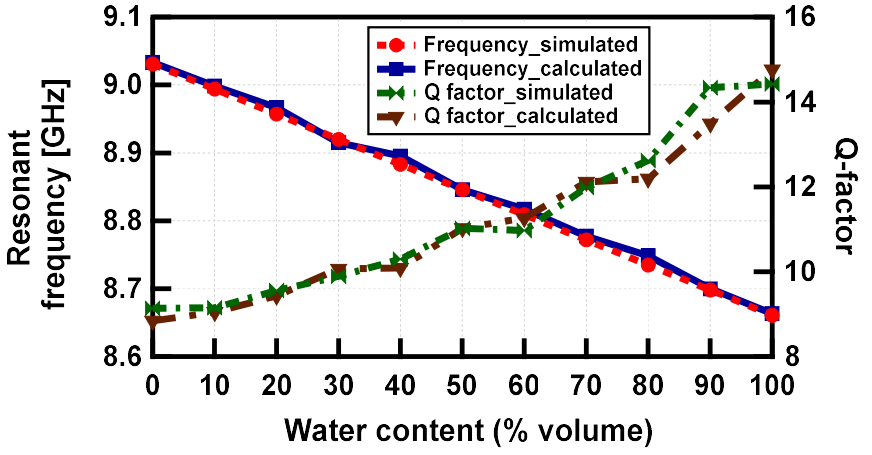

(c)

Fig. 21 Simulated and calculated resonance frequency and Q factor. (a) Ethanol-water mixture, (b) Methanol-water mixture, and (c) Acetone-water mixture.

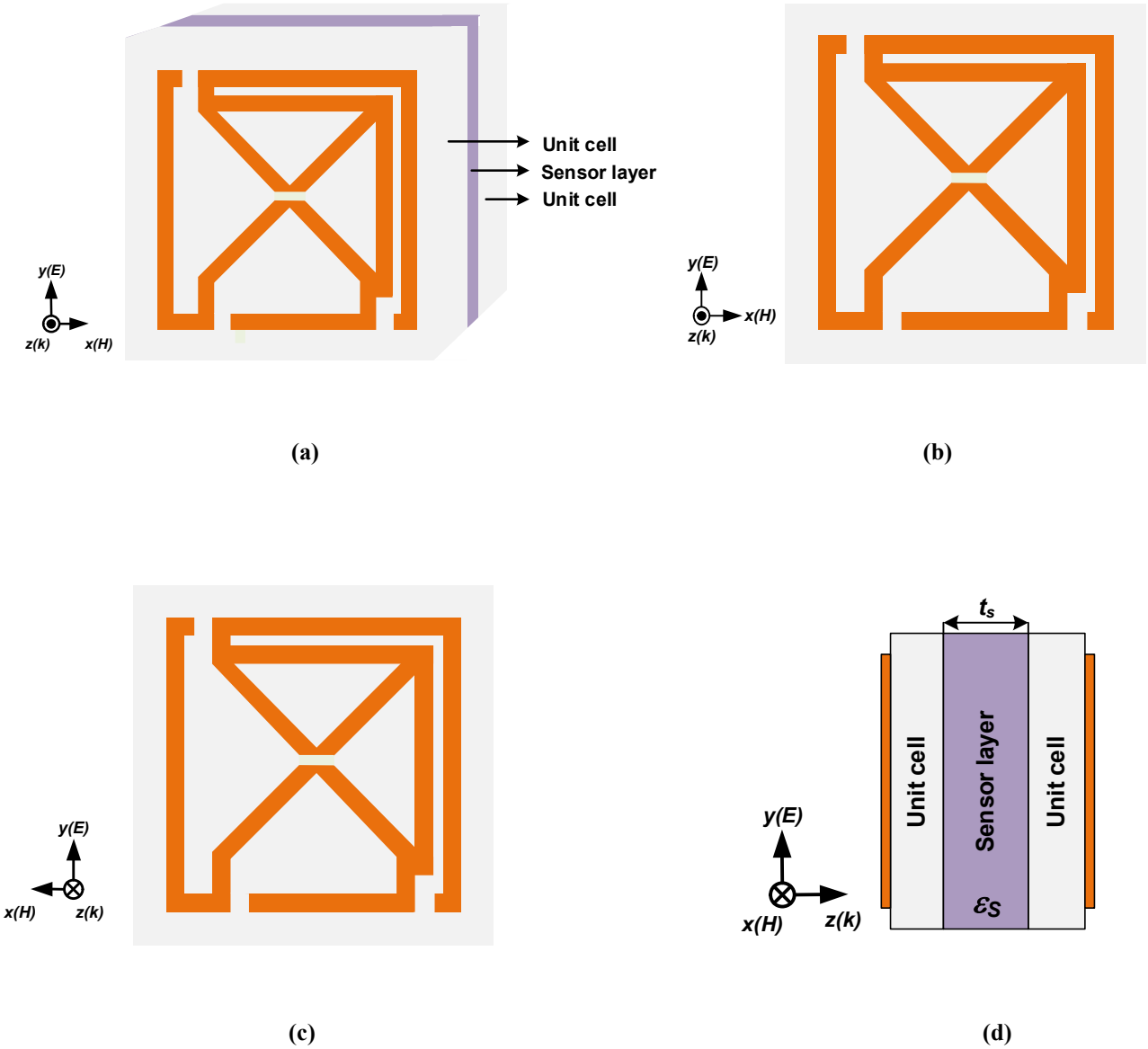

Fig. 22 Schematic diagram of the proposed NRI MTM based pressure sensor (a) Perspective view, (b) Front view, (c) Back view, and (d) Left view.

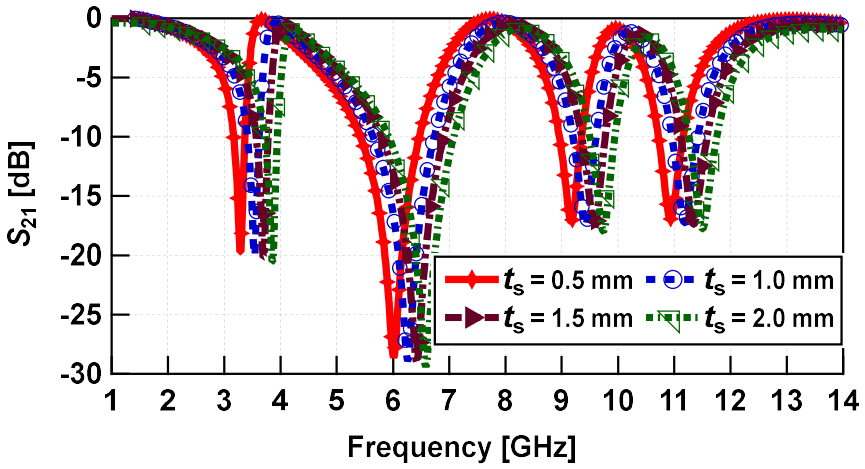

Fig. 23 S_{21} curves of the pressure sensor.